Semiconductor Physics, Quantum Electronics & Optoelectronics, 2026. V. 29, No 3. P. 361-366.

Hetero- and low-dimensional structures

Film heterophotocell with nanocluster subsystem

V.V. Kovalchuk[1*], D.O. Dyachok[2], D.V. Korban[3], K.V. Loskutov[2]

[1]*Odesa Technological University IT STEP, 65000 Odesa, Ukraine*
[2]*South Ukrainian National Pedagogical University named after K.D. Ushynsky, 65020 Odesa, Ukraine*
[3]*National Maritime Academy, 65020 Odesa, Ukraine*
Corresponding author e-mail: lslvvvas@ukr.net

Abstract. The effects associated with changes in the properties of a film heterojunction as a result of introducing a nanocluster subsystem into it are considered. Such a modified heterojunction exhibits spectral-inversion photovalve effect. A design of a photocell containing two series-connected opposite *p-n* junctions, photoactive in different spectral regions, is proposed.

Keywords: heterojunction, film, nanocluster, subsystem, properties, kinetics, irradiation, diffusion, photovalve effect.

https://doi.org/10.15407/spqeo29.03.361
PACS 62.23.St, 73.40.Lq

Manuscript received 14.11.25; revised version received 19.07.26; accepted for publication 16.09.26; published online 25.09.26.

1. Introduction

The study of properties of heterojunctions (HJs) deserves attention for solving problems of functional diagnostics of new generation devices. Such studies are relevant for developing effective photovalve elements [1–3].

The task of the work is to consider a possibility of manifestation of new properties of film HJs of the pCu$_2$S-nSi type, into which a cluster raster of subcolloidal dispersion in the form of a nanocluster subsystem (NCS) is introduced, and to determine the optimal operating modes of such a heterophotoelement.

2. Experimental

Transition from an individual atom to a macrostate is characterized by formation of structures such as quasi-molecular clusters and subcolloidal and colloidal nanoclusters (NCs), which are extensive in nature, since they consistently change their properties up to the properties of the corresponding macrosubstance [4]. The latter is very important to consider when using quasi-metallic NCs as a doping element for individual materials and heterostructures (HS) [5–10].

Quasi metallic centers (QMCs) in crystals (in particular, dielectric and ionic ones) with nanometer sizes (from 1 to 5 nm) can be formed using special technological methods (irradiation, heat treatment, action of optical radiation). Such QMCs represent an intermediate state between simple point defects (such as aggregates of F-centers) and macroscopic metal colloids.

Influence of the NCs of different sizes on the optical and some other properties of crystals ("red shift" of the color of the matrix material when the centers are enlarged, *etc.*) has been studied both theoretically and experimentally [11–13]. An analogy with different stages of a photographic process in silver halide materials and on semiconductors would be appropriate. Moreover, the size of NCs in a single-crystal matrix can be varied quite widely [4, 5].

Before depositing the Cu_2S film on the crystalline silicon substrate, a Si cluster pattern with an island structure was formed on the substrate by ion implantation.

By varying the NC formation rate and the substrate temperature, we were able to implant the cluster centers in the form of a nanocluster subsystem (NCS) of silicon into the pCu$_2$S-nSi-HJ. In this way, HJ of the pCu$_2$S-(Si-NCS)-nSi type was formed. For such HJ, "extensive" effects, in particular the spectral inversion effect, were observed.

It should be noted that the NCS in a heterojunction (HJ) can be also created by implanting transition metals, in particular, Fe, Ni, Co, and Cu [5]. Implantation of transition metals into the surface layer of Si is used to create silicides, to modify the electronic structure and to form magnetic nanostructures. Important aspects of this process are high diffusion rates, formation of deep recombination levels and synthesis of ferromagnetic phases. The latter is a good confirmation that the detected effects are to a greater extent due to the presence of NCS, and are not caused by the NCS material.

3. Results and discussion

The HJ considered in the work is formed from a Si NC. This material was chosen due to its advantage in terms of purity class over other materials that were at our disposal.

A common property of gate photovoltaic cells based on Si, Ge, Se, CdS and other materials is preservation of unchanged photovoltage polarity in the entire spectral active region, for which, according to the typical scheme of the gate photoeffect, the *n*-region is negatively charged with respect to the *p*-region under light illumination. At the same time, a possibility of reversing the polarity of the gate photovoltage by changing the illumination wavelength has been established.

The photoelectric element proposed in this work, which includes HJ with NCS, opens up new opportunities in solving a number of practical issues in optoelectronics related to the control and measurement of color temperatures of radiation sources, recognition of color images, *etc*.

One of the main recommendations is to introduce various impurities (Fe, Ni, Co, *etc*.) into the *p-n* junction region to provide traps and recombination centers of non-equilibrium electron-hole pairs. Another recommendation is to make a photovoltaic cell based on a complex HJ from different materials. This HJ contains two sequentially connected opposite *p-n* junctions photoactive in different spectral regions. In both cases, the photosensitivity of the device is low, and the spectral distribution of the photovoltaic effect is strongly asymmetric relative to the point of inversion of the polarity of the photovoltage. In the first variant, this is apparently due to the insufficiently high efficiency of the specified impurities as recombination centers. In the second variant this is due to the complication of optical-photoelectric conditions in a HJ with a sequential chain of transitions.

We have considered a possibility of creating a gate spectral-inversion heterophotocell in a configuration *p*Cu_2S-Si(NCP)-*n*Si, which structurally represents a combination of a half-film *p-n* heterojunction located at the contact between a *p*-type Cu_2S film and an *n*-type Si crystal, with an ultrafinely dispersed Si cluster raster (NCS), distributed in the junction plane. The cluster raster forms an “island” structure, which is organically included in the heterojunction structure and, in particular, is embedded in the copper sulfide film.

The technology of obtaining a spectrally inverted *p*Cu_2S-*n*Si-HJ photovoltaic cell is generally similar to that described in [4], the only difference being that manufacture of samples begins with implementation of

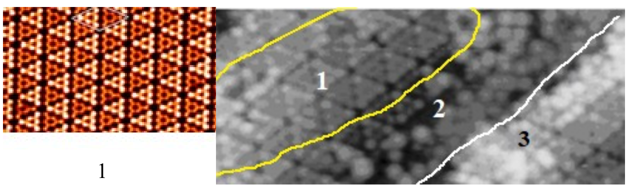

Fig. 1. High-resolution microphotograph (the image size 270×195 Å^2) of a Si(111) crystal surface: *1* –Si(111)-7×7 surface region in the filled state (the STM data show 12 adatoms and 6 rest atoms per a unit cell (7×7) [12]); *2* – micrographic NC silicon raster on the c-Si surface. It is a hierarchical two-dimensional large-scale texture combining microcrystalline structural elements and nanoclusters. The nanocluster pattern is created by metal-assisted etching, ion bombardment, and laser micro/nano structuring [13].

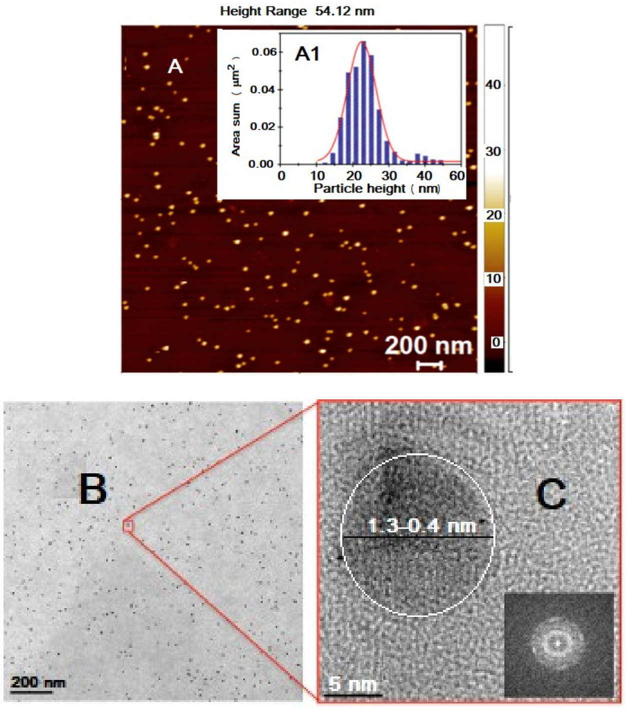

Fig. 2. Formation of NCs on a solid surface. Panel A is an AFM micrograph illustrating surface coverage of the Si NCs and their size distribution (inset, A1) [14]. Panels B and C are TEM micrographs of the Si NCs on the substrate [15].

a metal-cluster raster of subcolloidal dispersion with the size of individual particles not exceeding 20 Å on the surface of a Si washer (at a temperature of 100 °C). The HJ clustering operation was carried out by thermal evaporation in vacuum (~10^{-6} Torr) or by pyrolytic decomposition of compounds, in a mode that ensures formation of a subcolloidal metal monolayer on the control substrate, which is in the same conditions as the main substrate. This monolayer is clearly distinguishable with an electron microscope (Fig. 1).

Typically, sputtering of semiconductor materials is more difficult compared to metallic materials. However, the AFM results presented in Fig. 2 (panel A) indicate that Si nanoparticles with sizes of 10 to 20 nm are relatively easily deposited on the c-Si surface [14]. Fig. 2 (panels B and C) also present micrographs obtained using high-pressure transmission electron microscopy [15].

A schematic representation of a spectral inversion heterophotocell is shown in Fig. 3. The most important element of this design is a nanocluster raster. In the nanocluster raster, the NC dispersion degree is of particular importance. The result is a spectral inversion photocell with HJ having a (*p*Cu_2S-(Si-NCS)-*n*Si) NCS. Such a photocell has a clearly defined sensitivity distribution, which is shown in Fig. 4.

Operation of a spectral inversion photocell of the *p*Cu_2S-(Si-NCS)-*n*Si type is ensured by combining two essentially different mechanisms of the gate photoeffect in one HJ, separated by their spectral active regions. The first mechanism implements the well-known scheme of

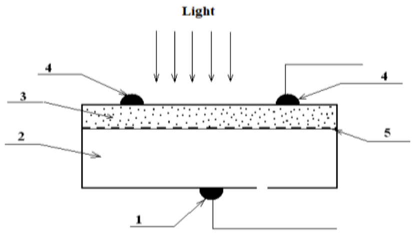

Fig. 3. Schematic diagram of a spectral-inversion heterophotocell pCu$_2$S-Si(NCS)-nSi: *1*, *4* – thin-layer contacts; *2* – silicon crystal; *3* – copper sulfide film; *5* – subcolloidal nanocluster array (NCS).

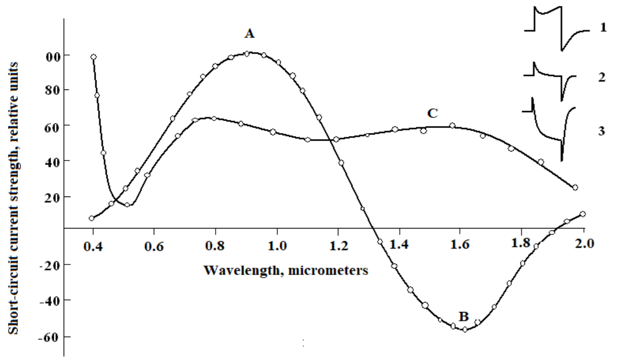

Fig. 4. Spectral distribution of the inversion photovalve effect of HJ with NCS – (pCu$_2$S-(Si-NCS)-nSi): A and B – regions of the normal and anomalous effect, respectively, C – optical absorption spectrum of the Cu$_2$S film. Plots (top right) of the photoresponse kinetics: *1* – in the region of the normal effect, *2* – at the inversion point, *3* – in the region of the anomalous effect.

the gate photoeffect in the *p-n* junction (Fig. 4A), according to which the *n*-region (silicon) is negatively charged under illumination. The spectral distribution of the photovoltaic effect in this case (Fig. 4A, 4B) corresponds to photoactive absorption of light in both materials Cu$_2$S and Si, which is facilitated by the pCu$_2$S-nSi – HJ zone diagram favorable for the photocell. The second mechanism (Fig. 4B) operates in clustered areas of HJ, *i.e.* where NCs are located. Its spectral characteristic corresponds to absorption of light by nanoparticles (Figs. 4B, 4C).

The result of the action of light is generation of photovoltage (photocurrent) in a direction opposite to that caused by an action of the first mechanism, *i.e.* Si is positive under an action of light from this spectral region, and Cu$_2$S is negative.

The mechanism of photoelectric effect in NCs is much more complex and does not reduce to a simple linear or single-stage “input-output” scheme. Although at the conceptual level, there is an optical signal at the input (photons) and an electric current at the output (electrons). The “input-output” model assumes a direct, instantaneous and proportional dependence of the result on the perturbation. In NCs (quantum dots), the photoeffect is a multistage quantum process with an internal “memory”, dependence on the size, shape and environment of the NC, and nonlinearity of the system [16].

To explain the principle of “input-output” action for the effect of solvation of nanoparticles (in our case, NCs) by holes (Fig. 4B), the Scheme 1 is proposed.

Scheme 1. “Input-Output” for the effect of solvation of NCs by holes.

[INPUT]
(Hole concentration in Cu$_2$S, NC properties)
↓
[CONTROLLING PROCESS]
(Local “salvation” by holes and formation of a dipole layer)
↓
[INTERNAL SYSTEM CHANGE]
(Band shift / Electrostatic bending)
↓
[OUTPUT]
(Lowering barrier, Decrease in work function,
Increase in electron current)

Explanation and detail of the circuit elements.

The circuit parameters are distributed as follows:

1. Input parameters (Input). Primary input: excess concentration of free holes in the Cu$_2$S *p*-film.

2. Transformation process (Black Box/System Operator). Diffusion of holes to the interface boundary and their accumulation around the NC (“salvation”). Formation of a double electric (dipole) sphere at the nanocontact. Change in the macroscopic potential at the interface, which causes a shift of the energy bands (band bending).

3. Output parameters (Output). Energy output: specific reduction in the height of the potential barrier. Functional output: effective reduction in the work function of an electron from NC. Kinetic output: sharp increase in the electron transmission coefficient (emission/transport intensity) into the *p*-region of the heterojunction.

The photoelectric effect on NCs changes its electronic structure. Potential wells and energy barriers are formed, and localized electron traps arise, which directly control the transport of current carriers.

At the nanometer scale, the process of electron emission or photocurrent generation depends on the geometric parameters of the NC. When the size of the NC decreases and becomes smaller than 5 nm, movement of electrons is limited in all three dimensions. In this case, the following processes occur: the band gap (E_g) of the silicon NC increases (up to 1.5…2.5 eV depending on the NC size. E_g = 1.12 eV for c-Si); the conduction (E_c) and valence (E_v) bands split into quantum levels; and energy barriers and local energy levels appear. For NCs with sizes up to 3 nm, the quantum energy levels in the conduction band (E_c) are located below or above the edges of the bulk substrate bands (within 0.20 eV). This creates specific conditions for charge injection [17].

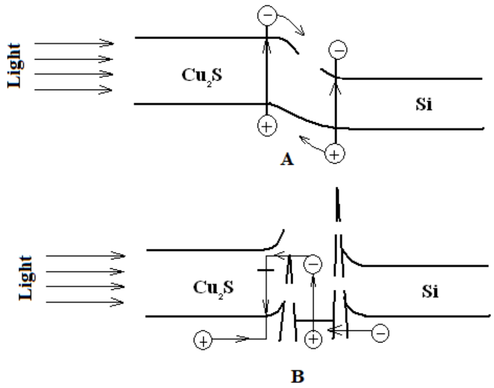

Fig. 5. Band energy diagrams: (A) of HJ free of NCs of the pCu$_2$S-nSi type and (B) HJ with NCs – pCu$_2$S-(Si-NCS)-nSi.

Near the NC, the energy situation also changes significantly. There is a substantial influence of the matrix environment [18]. At the interface between the NC and the matrix environment (*e.g.* SiO_2), the band diagram becomes complex. Here, the NC functions as a three-dimensional potential well for charge carriers, which is surrounded by high energy barriers of the matrix. This well for the SiO_2 matrix is equal to 3.1 eV for electrons and 4.7 eV for holes. Due to the small intrinsic capacitance of the NC, the impact of even one electron on the NC creates a powerful energy barrier (a Coulomb repulsion energy arises), which prevents capture of the next electron. A large number of surface states are formed directly near the NC surface. Traps for electrons and holes (unsaturated bonds of silicon or bonds with oxygen) arise creating deep and shallow energy levels within the band gap. These level capture charge carriers and block or enhance current.

Passivation of broken chemical bonds of silicon atoms on the surface of NCs *e.g.* with hydrogen atoms compensates for localized states from the band gap and equalizes the potential. The accumulated charge in the traps near the NCs creates local electric microfields that distort the energy bands of neighboring matrix regions changing the tunneling conditions (Fowler–Nordheim modes or direct tunneling). Controlled capture by electron traps is used in non-volatile memories. For example, the charge localized in a trap changes the threshold voltage of a transistor. This allows storing a logical bit of information for a long time [19].

According to calculations of the electronic structure of Si NCs by quantum chemistry methods [4], these nanoclusters tend to have a certain excess negative charge in equilibrium. This is a condition for NC stability and further growth up to colloidal sizes. Under such conditions, presence of a high concentration of holes in Cu_2S should lead to a kind of "solvation" of NCs by holes from the Cu_2S film, which results in a decrease in the effective work function of electrons from the NC to the HJ *p*-region (Fig. 5).

A photoexcited electron is moved from a NC deep into the Cu_2S film, where, most likely, it is captured on a highly developed system of electron adhesion levels in this quasi-monopolar semiconductor. Simultaneously with the photoexcitation of the first electron in the NC, another one tunnels from the Si valence band *etc*., *i.e.*, the process that constitutes the essence of the "feed in – feed out" scheme is reproduced.

The spectral activity region of the negative photovoltaic element defines the effective energy depth of the NCs at 0.8 eV. This parameter is of significant importance for spectral inversion of the photoeffect, since it provides tunnel contact with the valence band of silicon. When switching to a cluster raster with large-sized NCs (more than 20 Å), the "feed in – feed out" effect disappears, in other words, the spectral inversion photovoltaic effect is not observed.

This may be explained by extinction of the solvating factors that ensure the necessary "feed in – feed out" mechanism for the operation of the potential barrier profile around the NC, as a result of weakening of the Coulomb field of the large-sized NCs.

Direct confirmation of the mechanism of the spectral-inversion photovalve effect discussed above was obtained by parallel measurements of the kinetics of photoconductivity in the base region of the photocell – the Si plate. When the pCu$_2$S-(Si-NCS)-nSi photocell was illuminated with light from the spectral region correspon-ding to creation of anomalous photovalve effect (IRS-3 filter), the photoresponse of the base region of the element was significantly smaller when the photocell was open (idle mode) than in the case of a short circuit (Fig. 6).

For a pCu$_2$S-nSi photocell that does not contain NCs, the behavior in similar situations will be opposite in the entire active region of the spectrum. The results obtained by us are easy to interpret by comparing two mechanisms of the photovalve effect – ordinary and "feed in – feed out". In the latter case, extraction of electrons from silicon on the NCs leads to a decrease in the photocurrent in the base circuit. Naturally, in the short-circuit current mode, such observations are less pronounced due to the continuous restoration of the concentration of non-equilibrium electrons in silicon from the external circuit.

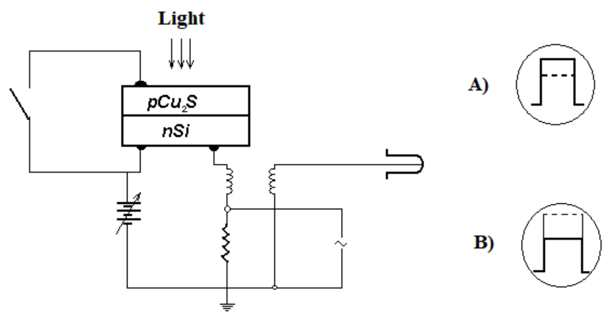

Fig. 6. Scheme of observation of the kinetics of photo-conductivity (IRS-3 filter) in the low-resistance base layer of the photocell and kinetic diagrams of photocurrent (the dotted line indicates short-circuit mode of the photocell): A) pCu$_2$S-nSi – photocell; B) pCu$_2$S-(Si-NCS)-nSi – photocell.

There are also other considerations that confirm the proposed mechanism of spectral inversion of the photovalve effect in pCu$_2$S-(Si-NCS)-nSi HJ. The fact is that in this situation, it would be possible to assume participation of Schottky microbarriers at the "NC-matrix material" interface in the spectral-inverted effect. These microbarriers create an electric field opposite to the barrier field in the heterojunction and provide an anomalous photovalve effect. However, the latter is unlikely for the following reasons. It is known that significant contact barriers are formed as a result of transition of $\sim 10^{15}$ electrons from one material to another, which causes a distortion of energy bands. Emergence of Schottky barriers in the place of contact of the NCs with the matrix substance is impossible due to the small NCs size.

Theoretical estimates presented in [4, 5] show that ionization or capture of even one electron in the NCS leads to a sharp change in the position of the Fermi level of the NC by units of eV. On the one hand, this fact significantly complicates further electron exchange between the NC and the matrix material. This is absolutely not enough to distort the energy bands of the matrix crystal in this region due to the small concentration of charge involved in the exchange.

The insignificance of the role of Schottky barriers between the NC and the matrix material also follows from the experimental facts themselves. At NC sizes up to 20 Å, the role of the Schottky barriers should increase up to formation of a mesh structure at the interface. That is, one should expect dominance of the anomalous photovalve effect or even complete transformation of the photovalve effect in the pCu$_2$S-(Si-NCS)-nSi HJ from normal to anomalous one. But this does not actually happen, since the photovalve effect not only does not increase, but, on the contrary, completely disappears with an increase in the NC size to hundreds or more angstroms. For example, the diffusion coefficient of Ni in Si at temperatures of ~100 °C is negligibly small. In other words, atomic doping of Si with nickel during obtaining pCu$_2$S-(Si-NCS)-nSi – photovoltaic cells is effective.

4. Conclusions

A technology for changing the properties of a film HJ of the pCu$_2$S-nSi type by introducing a cluster raster of subcolloidal dispersion in the form of NCS, which provides a smooth band-energy transition profile, is proposed. Such structure is suggested to use as a base for photovalve energy converters. The optimal operation modes of such heterophotocell are determined. The structure of a HJ can be changed by implanting (introducing or depositing) a cluster raster of an island structure at the interface or in one of the HJ layers. This is an effective method of spatial and energetic modification of the HJ properties. This approach is actively used in modern nanoelectronics, photovoltaics, and LED technologies.

Varying the NC formation rate and substrate temperature opens up a possibility of implanting NCs with sizes from 10 to 150 Å. In our opinion, manifestation of the spectral inversion effect observed in GPs with NCPs is extensive in nature, *i.e.* this effect directly depends on the number of absorbed photons, NCS morphology, defect concentration, and NC size and geometry.

The presented research results deserve attention in solving problems of modern functional diagnostics of devices with NCS as well as in the development of photovalve elements.

The spectral-inversion photodetector described in this work, in addition to its independent application, can be used in designs with nanostructures [3, 4], in particular, when creating optocouplers, such as bichromatic LEDs with controlled emission frequency.

References

1. Sabbatucci L., Salvat F. Theory and calculation of the atomic photoeffect. *Radiat. Phys. Chem.* 2016. **121**. P. 122–140. https://doi.org/10.1016/j.radphyschem.2015.10.021.
2. Li Q., Bi Sh., Asare-Yeboah K. High performance vertical resonant photo-effect-transistor with an all-around OLED-gate for ultra-electromagnetic stability. *ACS Nano.* 2019. **13**, No 7. P. 8425–8432. https://doi.org/10.1021/acsnano.9b04163.
3. Kovalchuk V.V. Heterophotocell based on super-line photoventil effect. *J. Phys. Electron*. 2020. **28**, No 1. P. 61–68. https://doi.org/10.15421/332011.
4. Kovalchuk V.V. Deep submicron particles in a solid matrix environment. *Metrology & Instruments*. 2020. **5**. P. 56–60. https://doi.org/10.33955/2307-2180.
5. Saga K., Ohno R., Shibata D. *et al.* Behavior of transition metals penetrating silicon substrate through SiO_2 and Si_3N_4 films by arsenic ion implantation and annealing. *ECS J. Solid State Sci. Technol.* 2015. **4**, No 5. P. 131–136. https://doi.org/10.1149/2.0061505jss.
6. Kovalchuk V.V., Popriaha D.O. Optical properties of the semiconductor nanoclusters. *Technium: Rom. J. Appl. Sci. Technol.*·2025. **28**. P. 35–42. https://doi.org/10.47577/technium.v28i.12625.
7. Mishra P.K., Dash A., Rini E.G. *et al.* Defects altered *n*/*p*-type Fe/Ga modified ZnO for photosensing applications. *Mater. Today Commun.* 2023. **36**. P. 106371. https://doi.org/10.1016/j.mtcomm.2023.106371.
8. Xu J., Zhou H., Zhang Y. *et al.* Copper nanoclusters-based fluorescent sensor array to identify metal ions and dissolved organic matter. *J. Hazard. Mater.* 2022. **428**. P. 128158. https://doi.org/10.1016/j.jhazmat.2021.128158.
9. Grigorchuk N. Size and shape effect on optical conductivity of metal nanoparticles. *EPL*. 2018. **121**, No 6. P. 67003–67008. https://doi.org/10.1209/0295-5075/121/67003.
10. Tuğay E., Turan R. Investigation of photoluminescence mechanisms from SiO_2/Si:SiO_2/SiO_2 structures in weak quantum confined regime by deconvolution of photoluminescence spectra. *Nanosci. Nanotechnol.* 2016. **16**, No 4. P. 4052–4064. https://doi.org/10.1166/jnn.2016.10863.

11. Piven Oleksandr B., Piven Oleh B., Lopatkin Y.M. Peculiarities of crystallization of amorphous silver at 77 K in conditions of laser Herschel effect. *J. Nano- Electron. Phys.* 2019. **11**, No 3. P. 03023. https://doi.org/10.21272/jnep.11(3).03023.
12. Wang Y.-L., Guo H.-M., Qin Z.-H. *et al.* Toward a detailed understanding of Si(111)-7X7 surface and adsorbed Ge nanostructures: Fabrications, structures, and calculations. *J. Nanomater*. 2008. Art. ID 874213. https://doi.org/10.1155/2008/874213.
13. Seo J., Pearson D., Bradley R., Kim J-S. Nanoscale pattern formation on silicon surfaces bombarded with a krypton ion beam: Experiments and simulations. *J. Phys.: Condens. Matter*. 2022. **34**. P. 265001. https://doi.org/10.1088/1361-648X/ac64df.
14. Schierning G., Theissmann R., Wiggers H. *et al.* Microcrystalline silicon formation by silicon nanoparticles. *J. Appl. Phys.* 2008. **103**. P. 084305. https://doi.org/10.1063/1.2903908.
15. Cassidy C., Singh V., Hawash Z. *et al*. Size-controlled deposition of Ag and Si nanoparticle structures with gas-aggregated sputtering. *Mater. Res. Soc. Symp. Proc.* 2013. **1546**. https://doi.org/10.1557/opl.2013.658.
16. Tate N., Miyata Y., Sakai S. *et al*. Quantitative analysis of nonlinear optical input/output of a quantum-dot network based on the echo state property. *Opt. Express*. 2022. **30**. 14669–14676. https://doi.org/10.1364/OE.450132.
17. Bisri S.Z. Charge carrier injection and extraction of colloidal quantum dot assemblies: A perspective for optoelectronic devices. *J. Inform. Display*. 2025. **26**. P. 109–130. https://doi.org/10.1080/15980316.2025.2501386.
18. Bratus O., Evtukh A. Electrical properties of composite films with silicon nanocrystals in the insulating matrix. *Adv. Mater. Res.* 2014. **854**. P. 105–110. https://doi.org/10.4028/www.scientific.net/AMR.854.105.
19. Leroy Y., Cordan A.S., Leriche B. Modeling of single electron charging in nanocrystal memories. *IETE J. Res.* 2006. **52**, No 5. P. 327–332. https://doi.org/10.1080/03772063.2006.11416472.

Authors and CV

Volodymyr Kovalchuk, DSc, Professor at the Odesa Technological University IT STEP. Author of more than 400 publications. The area of his research interests is physical properties of nanomaterials.
E-mail: kovalchuk_vv@itstep.org,
https:// orcid.org/0000-0001-7460-8092

Dmytro Dyachok, PhD, Associate Professor, Department Head at the South Ukrainian National Pedagogical University named after K.D. Ushynsky. Author of more than 30 publications. The area of his research interests is physical properties of nanomaterials.
E-mail: dyachok13@gmail.com,
https://orcid.org/0000-0002-9036-1138

Dmytro Korban, PhD, Associate Professor, National Maritime Academy (Odesa, Ukraine). Author of more than 100 publications. The area of his research interests is the practical use of electronic devices based on nanomaterials.
E-mail: korbandmv@gmail.com,
https://orcid.org/0000000267982526

Konstantin Loskutov, PhD Student at the South Ukrainian National Pedagogical University named after K.D. Ushynsky. Author of 4 publications. The area of her research interests is physical properties of nanomaterials.
E-mail: lslvvvas@ukr.net
https://orcid.org/0009-0003-8398-9589

Authors' contributions

Kovalchuk V.V.: conceptualization, supervision, project administration, writing – review & editing.
Korban D.V.: investigation, resources.
Dyachok D.O.: investigation, formal analysis, visualization, writing – original draft.
Loskutov K.V.: investigation, resources, writing – original draft.

Плівковий гетерофотоелемент з нанокластерною підсистемою

В.В. Ковальчук, Д.О. Дячок, Д.В. Корбан, К.В. Лоскутов

Анотація. Розглянуто ефекти, пов'язані зі зміною властивостей плівкового гетеропереходу в результаті введення у нього нанокластерної підсистеми. Такий модифікований гетероперехід виявляє спектрально-інверсійний фотовентильний ефект. Запропоновано конструкцію фотоелемента, що містить два послідовно з'єднаних *p-n*-переходи зустрічної дії, фотоактивні в різних областях спектра.

Ключові слова: гетероперехід, плівка, нанокластер, підсистема, властивості, кінетика, опромінення, дифузія, фотовентильний ефект.